the plasma may also contribute to a reduction in the Auger recombination rate as a result of the action of the Pauli exclusion principle in limiting the number of available final states. It is possible that this latter effect is evident in the fact that at the reduced (but still degenerate) density of 1.4×10^{20} cm^{-3}, we find that the rate constant is larger by a factor of approximately 1.8 than at 3.4×10^{20} cm^{-3} (Fig. 2).

In summary, we have demonstrated the utility of picosecond optical pulses for the measurement of fast nonradiative band-to-band Auger recombination of high-density semiconductor plasmas. The high intensity and short duration of picosecond pulses allows the study of recombination kinetics in a density and time regime where the Auger effect dominates all other recombination processes. Furthermore, it is possible to determine the rate constant in a time interval which is short compared to diffusion times.

[1]R. Beattie and P. T. Landsberg, Proc. Roy. Soc. London, Ser. A 249, 16 (1959).
[2]L. Huldt, Phys. Status Solidi (a) 24, 221 (1974).
[3]L. R. Weisberg, J. Appl. Phys. 39, 6096 (1968).
[4]W. Rosenthal, Solid State Commun. 13, 1215 (1973).
[5]L. M. Blinov, E. A. Bobrova, V. S. Vavilov, and G. N. Galkin, Fiz. Tverd. Tela 9, 3221 (1967) [Sov. Phys. Solid State 9, 2537 (1968)].
[6]R. Conradt and W. Waidelich, Phys. Rev. Lett. 20, 8 (1968).
[7]R. Conradt and J. Aengenheister, Solid State Commun. 10, 321 (1972).
[8]N. G. Nilsson and K. G. Svantesson, Solid State Commun. 11, 155 (1972); N. G. Nilsson, Phys. Scr. 8, 165 (1973).
[9]D. H. Auston and C. V. Shank, Phys. Rev. Lett. 32, 1120 (1974).
[10]W. C. Dash and R. Newman, Phys. Rev. 99, 1151 (1955).
[11]R. Newman and W. W. Tyler, Phys. Rev. 105, 885 (1957); J. I. Pankove and P. Aigran, Phys. Rev. 126, 956 (1962).

Angle and Energy Dependence of Photoemission from NaCl and KCl Single Crystals*

F.-J. Himpsel and W. Steinmann
Sektion Physik der Universität München, München, Germany
(Received 18 August 1975)

The dependence of photoemission on the azimuthal emission angle at fixed polar angle of 45° was measured for the (100) face of NaCl and KCl single crystal cleaved *in situ*. The initial- and final-state energy was scanned using synchrotron radiation. Strong variations of the angular pattern are observed for different final-state energies. Below the electron-electron scattering threshold the pattern depends only on the final-state energy. Electron-phonon scattering can account for this fact.

Experimental data suitable for testing band-structure calculations for alkali halides are remarkably scarce in view of the enormous number of experiments which have been performed with these fundamental compounds. The reason for this is the dominating influence of excitons on the optical spectra and the excellent insulating properties which, so far, have restricted photoelectron spectroscopy to samples of thin evaporated films.

In this Letter we report on the first ultraviolet photoemission experiment with bulk alkali halide single crystals. This allows us to measure the angular distribution of the photoelectrons, as has been done before with metals and semiconductors.[1-7] Although our investigation was incomplete since the polar angle could not be varied, the data yield considerably more detailed information than former experiments which integrated over all angles. They show that angle-resolved photoelectron spectroscopy on alkali halides is possible and may prove to be a promising method of investigating the electronic structure in detail, if the problem of matching the wave functions at the surface can be attacked successfully.[8]

We have used the synchrotron radiation of DESY as a light source. This enabled us to vary the photon energy continuously and to scan either the initial- or the final-state energy of the photoelectrons. The experimental equipment has been described prevously.[9,10] It consisted essentially of a normal-incidence monochromator with 2-Å resolution and an ultrahigh-vacuum sample chamber with a base pressure in the 10^{-11}-Torr range.

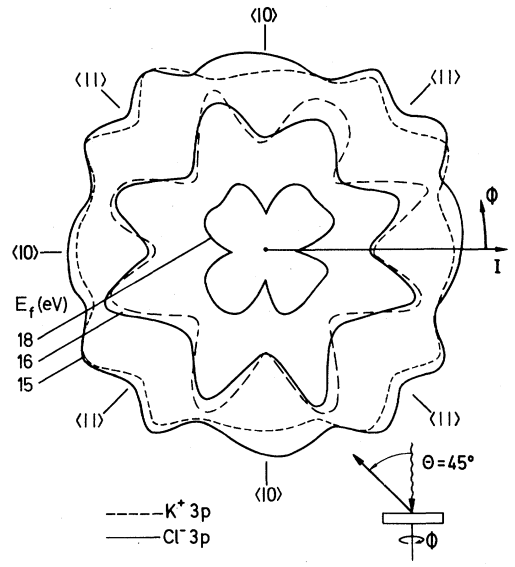

FIG. 1. Polar diagram of the photoemission intensity I as a function of azimuth φ for the KCl (100) face at fixed polar angle θ of 45° for three final-state energies (15, 16, and 18 eV above the top of the valence band) and two initial-state energies (Cl^- 3p valence band and K^+ 3p core level). ⟨10⟩ marks the orientation in which the [10] surface vector lies in the emission plane.

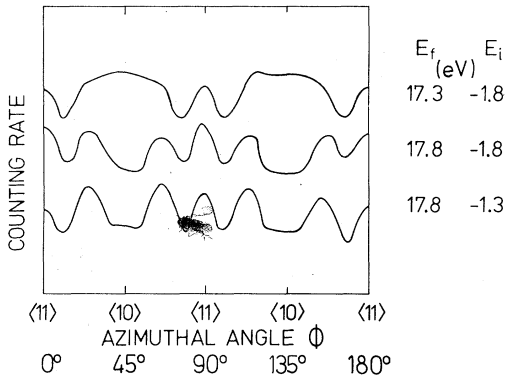

FIG. 2. Dependence of photocurrent on azimuth for the NaCl (100) face for the two initial-state energies E_i in the valence band and two final-state energies E_f. The zero line of the central curve is the bottom of the frame. The zero lines of the higher and lower curves have been shifted for clarity.

NaCl and KCl single crystals were mounted on a rotary-motion feedthrough. The axis of rotation coincided with the direction of the incident light. The crystals were cleaved *in vacuo*, the cleavage plane (100) being normal to the incident light beam. Photoelectrons were analyzed at a constant takeoff angle of 45° towards the normal of the surface (polar angle). The emission plane, defined by the emission direction and the normal of the surface, also contained the electric field vector of the incident light. The azimuthal emission angle was varied with respect to the crystal by turning the sample around its normal (see inset, Fig. 1). The electron energy analyzer of the filter-lens type had an energy resolution of better than 0.2 eV and an angular acceptance of 3°.

A serious problem is posed by the insulating properties of the crystals which result in excessive charging. We have overcome this difficulty by compensating the photoelectron current with thermal electrons from a heated tungsten filament located at a distance of 7 cm in front of the sample. Backscattered compensation electrons formed a peak about 1 eV wide at the bottom of the energy distribution. No background was found for kinetic energies higher than 2 eV. The experimental results proved that spatial and temporal fluctuations of the potential at the photoemitting part of the sample could be kept below 0.5 eV by this compensation.

Residual magnetic fields were held below 50 mG by Mumetal shielding. Additionally applied fields of the magnitude of the ambient earth field did not change the shape of the angular patterns. For electron energies below 5 eV at most, an angular offset of a few degrees and an overall decrease of the intensity could be detected. This can be explained by the limited angular acceptance of the analyzer combined with the size of the illuminated spot and the sample-to-analyzer distance. It ensures that any electron that has been deflected appreciably is not registered. The arrangement was tested for possible artifacts in the azimuthal photoemission pattern with a piece of glass as a sample. No variation of the intensity with azimuthal angle was detected in this test.

Examples of the azimuthal patterns from KCl at fixed electron energies are given in Fig. 1. Pronounced changes of the pattern with photon energy are observed. Note that photoemission from the K^+ 3p core level yields the same pattern as from the Cl^- 3p valence band if the final-state electron energy is the same. This holds also for different initial states within the valence band, as is shown in Fig. 2 for a restricted set of data from NaCl: A change of 0.5 eV in the initial energy does not produce any noticeable difference in the azimuthal pattern while the same

change in the final-state energy inverts the minimum in the (10) direction. Within the limits of our resolution we have found that the NaCl angular pattern depends only on the final-state energy in the whole range below 19 eV. For higher energies, however, the pattern shows a significant dependence on both initial- and final-state energy.

This behavior can be explained by electron-phonon scattering below the onset of electron-electron scattering at final-state energies exceeding twice the band-gap energy E_g ($E_g \approx 8.5$ eV for NaCl[11]). Below this threshold the escape depth of the photoelectrons is large compared to the electron-phonon scattering length. This leads to an extraordinarily high photoelectric yield exceeding 0.5 electron per photon[12] which has been explained by a random-walk process. Consequently a photoelectron escaping from the sample has undergone several phonon-scattering processes and lost completely the correlation to its initial position in k space. The angular distribution is determined by the density of final states. Above the electron-electron-scattering threshold the escape depth decreases within a few eV to values smaller than the electron-phonon-scattering length.[13] The number of high-energy photoelectrons is drastically reduced, but those which escape have not been scattered by either electrons or phonons. Their directions of emission depend on the k vector of the initial state even though the situation is complicated by the fact that at most the component of the k vector parallel to the surface is conserved during the escape.

Most of the electrons excited to these high final-state energies will undergo electron-electron scattering before they reach the surface, thereby loosing an amount of energy $E_s \geq E_g$ and populating conduction-band states of energy $E_f' = E_f - E_s$. We have found that the azimuthal pattern of these scattered electrons is the same as that of the valence electrons excited directly to the final-state energy E_f'.

In Fig. 3 is shown how the azimuthal pattern changes with final-state energy over the range investigated. The data contain the relevant information about the density of final states 4–13 eV above the bottom of the conduction band corresponding to the angles of emission. In general, the relation between Bloch states in the crystal and a plane wave outside has to be established by matching the wave functions at the boundary. This is a problem similar to the one encountered in low-energy-electron-diffraction intensity calculations. A solution requires some foreknowledge of the conduction-band states and wave functions. Nearly-free-electron models[14] may fail to give a complete description because of the d bands. If one neglects these complications and tries a rather crude approximation, assuming that the k direction in the crystal is the same as outside, one can compare the variation of the intensity in, e.g., the ⟨10⟩ direction with the density of states along the Σ axis. As can be seen in Fig. 3, there is a maximum in the ⟨10⟩ direction up to a final-state energy of 16 eV which changes into a minimum between 18 and 20 eV. This behavior can be accounted for by a band-structure calculation[15] which shows, along the Σ axis, a region with high density of flat bands up to 16 eV and the onset of a parabolic band at 17 eV. The investigation of valence-band states is possible by studying the angular distributions at final-state energies above 20 eV where the results depend also on the initial states.

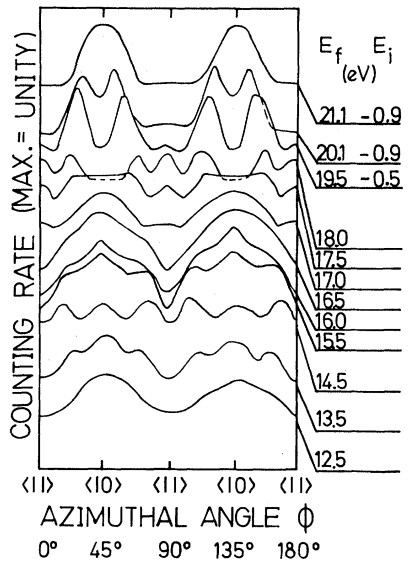

FIG. 3. Azimuthal patterns of the valence-band photoemission from a NaCl (100) face. The zero line is shifted proportional to the final-state energy as indicated on the right-hand side of the figure. The curves are normalized with respect to their maximum value.

We thank B. Feuerbacher, E. E. Koch, H. W. Rudolf, V. Saile, and N. Schwentner for valuable discussions and M. Skibowski for support of the project.

*Work supported by Deutsches Elektronen-Synchro-

ton, Hamburg, and by Bundesministerium für Forschung and Technologie, Bonn.

[1]B. Feuerbacher and B. Fitton, Phys. Rev. Lett. 30, 923 (1973).

[2]N. V. Smith and M. M. Traum, Phys. Rev. Lett. 31, 1247 (1973).

[3]M. M. Traum, N. V. Smith, and F. J. Di Salvo, Phys. Rev. Lett. 32, 1241 (1974).

[4]J. E. Rowe, M. M. Traum, and N. V. Smith, Phys. Rev. Lett. 33, 1333 (1974).

[5]R. R. Turtle and T. A. Calcott, Phys. Rev. Lett. 34, 86 (1975).

[6]W. F. Egelhoff and D. L. Perry, Phys. Rev. Lett. 34, 93 (1975).

[7]N. V. Smith and M. M. Traum, Phys. Rev. B 11, 2087 (1975).

[8]D. L. Rogers and C. Y. Fong, Phys. Rev. Lett. 34, 660 (1975).

[9]N. Schwentner, A. Harmsen, E. E. Koch, V. Saile, and M. Skibowski, in *Vacuum Ultraviolet Radiation Physics*, edited by E. E. Koch, R. Haensel, and C. Kunz (Pergamon, New York, 1974), p. 792.

[10]N. Schwentner, F. J. Himpsel, V. Saile, M. Skibowski, W. Steinmann, and E. E. Koch, Phys. Rev. Lett. 34, 528 (1975).

[11]R. T. Poole, J. G. Jenkin, J. Liesegang, and R. C. C. Leckey, Phys. Rev. B 11, 5179 (1975).

[12]P. H. Metzger, J. Phys. Chem. Solids 26, 1879 (1965).

[13]J. Llacer and E. L. Garwin, J. Appl. Phys. 40, 2766 (1969).

[14]E. G. McRae, Surf. Sci. 44, 321 (1974).

[15]C. Y. Fong and M. L. Cohen, Phys. Rev. Lett. 21, 22 (1968).

Nonresonant ($\Delta m = 0$) Ultrasonic Coupling to Spin Quadrupole Modes in a Dilute Paramagnetic System*

Marjorie Passini Yuhas, Peter A. Fedders, J. G. Miller, and D. I. Bolef
Laboratory for Ultrasonics, Department of Physics, Washington University, St. Louis, Missouri 63130
(Received 10 July 1975)

We report the first use of low-frequency, nonresonant ($\Delta m = 0$) ultrasound to investigate the dominant spin-lattice relaxation processes in dilute paramagnetic systems. A theory of the interaction of paramagnetic spins with ultrasonic waves is presented which emphasizes the coupling of acoustic waves to $\langle S_z^2 - \frac{1}{3}S(S+1)\rangle$, the $l=2$, $m=0$ spin quadrupole. Results of experiments over the range 4.2 to 30 K, using 30-MHz longitudinal ultrasonic waves in single-crystal MgO:Fe^{2+}, are consistent with theoretical predictions.

We demonstrate the feasibility of coupling externally generated ultrasonic phonons to electron spins in a dilute paramagnetic system by means of low-frequency, nonresonant, absorption methods rather than by conventional high-frequency, resonant, ultrasonic methods. Results from low-frequency paramagnetic absorption experiments on the system MgO:Fe^{2+} are reported here and are compared with theoretical predictions for nonresonant ultrasonic absorption. By low frequency we mean frequencies that are much less than any resonant frequency of the spin system but are still comparable to spin-relaxation rates. Nonresonant acoustic experiments such as the one described in this Letter can be of value in studying intrinsic spin-relaxation rates in systems in which resonant frequencies cannot be reached or in systems in which inhomogeneous broadening masks intrinsic linewidths.

We consider a single spin of magnitude S in a cubic environment with an extrernally applied magnetic field $\vec{H}_0$. In this case the irreducible tensor spin operators A_{lm}, where $|m| \leq l$ and $0 \leq l \leq 2S$, form the most convenient complete set of $(2S+1)^2$ spin operators.[1] In the high-temperature limit the thermal averages of the A_{lm}'s correspond to the diagonalized normal modes of the spin even in the presence of spin-lattice relaxation.[2]

Since acoustic strains e_{ij} are second-rank tensors, they couple to the quadrupole ($l=2$ multipole) modes in a way which can be written as

$$\mathcal{H}_{s\text{-}p} = \sum_{m,\, i \leq j} f_{2,m}(i,j) e_{ij} A_{2m}, \tag{1}$$

where the f's are the coupling constants. This particular way of writing the Hamiltonian emphasizes the coupling of the acoustic modes (represented by e_{ij}) to the spin modes (represented by A_{2m}).